

Ferromagnetic Copper(II) Complex Containing Ferrocenecarboxylato Bridging Ligands

Concepción López,^{*,†} Ramon Costa,^{*,†} Francesc Illas,[‡] Elies Molins,[§] and Enric Espinosa[§]

Departament de Química Inorgànica and Departament de Química Física, Facultat de Química, Universitat de Barcelona, Martí i Franquès 1-11, 08028-Barcelona, Spain, and Institut de Ciència de Materials de Barcelona, CSIC, Campus Universitari de Bellaterra, 08193-Cerdanyola, Spain

Received May 17, 2000

The synthesis and characterization of the copper(II) complex $[\text{Cu}_2(\text{dpt})_2\{(\mu\text{-O}_2\text{C})[(\eta^5\text{-C}_5\text{H}_4)\text{Fe}(\eta^5\text{-C}_5\text{H}_5)]\}_2](\text{ClO}_4)_2$ (**1**), where dpt = dipropylentriamine, are reported, and its structure was determined by single-crystal X-ray analysis. The compound crystallizes in the monoclinic system, space group $P2_1/n$, with $a = 9.920(2)$ Å, $b = 12.925(2)$ Å, $c = 15.768(3)$ Å, $\beta = 93.17(1)^\circ$, and $Z = 2$. The cationic part of **1** shows a tetrametallic core in which two ferrocenecarboxylato groups act as (*O,O'*) bridging ligands between two copper(II) ions with a square-pyramidal environment. Susceptibility measurements on this compound indicate a ferromagnetic, albeit weak, coupling between the two paramagnetic centers, with best-fit values of $J = +2.5(3)$ cm⁻¹ and $g_{\text{iso}} = 2.12(1)$. Magnetostructural correlations can be qualitatively explained on the basis of the topology of their chairlike core. A quantitative investigation has been performed by means of ab initio density functional theory based calculations in the broken-symmetry approach.

Introduction

The study of heteropolynuclear complexes containing ferrocenyl units has attracted a great interest in past years, since the presence of proximal metals in different environments, oxidation numbers, and spin states may influence their mutual cooperation in a wide variety of processes.^{1–10} Nevertheless, the number of articles focused on polymetallic copper(II) complexes containing ferrocenecarboxylate(–I) anions as ligands is rather scarce. Only four articles have been published in this field.^{11–14} The first one was reported in 1985 and deals with the dimeric complex $[\text{Cu}_2(\text{thf})_2\{(\mu\text{-O}_2\text{C})[(\eta^5\text{-C}_5\text{H}_4)\text{Fe}(\eta^5\text{-C}_5\text{H}_5)]\}_4] \cdot (\text{thf})$ in which the

four ferrocenecarboxylate anions act as (*O,O'*) bridging groups, leading to a cage-like core typical of the copper(II) carboxylate adducts. A few years later, Abuhijleh and Woods^{12,13} reported the syntheses and X-ray crystal structure of five neutral dimetallic complexes of the general formula $[\text{Cu}(\text{L})_2\{(\text{O}_2\text{C})[(\eta^5\text{-C}_5\text{H}_4)\text{Fe}(\eta^5\text{-C}_5\text{H}_5)]\}_2]$ (L = pyridine or imidazole derivatives) where the ferrocenecarboxylate anions act as monodentate or chelating groups. More recently, $[\text{Cu}_2(\text{bpy})_2\{(\mu\text{-O}_2\text{C})[(\eta^5\text{-C}_5\text{H}_4)\text{Fe}(\eta^5\text{-C}_5\text{H}_5)]\}_2](\text{ClO}_4)(\text{CH}_3\text{OH})^+$ and $[\text{Cu}_2(\text{bpy})_2\{(\mu\text{-O}_2\text{C})[(\eta^5\text{-C}_5\text{H}_4)\text{Fe}(\eta^5\text{-C}_5\text{H}_5)]\}_2(\text{CH}_3\text{OH})_2]^{2+}$ cations containing two terminal bipyridyl ligands and two (*O,O'*) bridging ferrocenecarboxylate ligands have also been synthesized and their electrochemical and magnetic properties reported.¹⁴

Previous experiences with copper(II) polynuclear systems showed that the use of tridentate amines induces pentacoordination around the metal centers.^{15,16} Our recent work with ferrocenecarboxylate compounds¹⁴ leads us to expect that these anions could occupy the two remaining coordination sites acting as bidentate bridging ligands, leading to polynuclear systems with superexchange interactions. The intensity and sign of J can be tuned by modifying the geometry of the copper(II) coordination sphere,^{17,18} which varies from square-pyramidal (sp) to trigonal-bipyramidal (tbp) depending on the presence of N substituents in the blocking triamines: the bulkier the substituents, the closer the geometry to a trigonal bipyramid is. Nevertheless, the steric effect of the ferrocenyl moieties may affect these tendencies.

On these bases, we decided to study whether the incorporation of tridentate alkylic N-donor ligands in the coordination sphere of the copper(II) could be important for modifying the geometric

* To whom correspondence should be addressed. Phone (+34) 934 021 265. Fax: (+34) 934 907 725. E-mail: clopez@kripto.qi.ub.es. E-mail: rcosta@kripto.qi.ub.es.

[†] Departament de Química Inorgànica, Universitat de Barcelona.

[‡] Departament de Química Física, Universitat de Barcelona.

[§] Institut de Ciència de Materials de Barcelona.

- (1) Togni, A. *Ferrocenes, Homogeneous Catalysis, Organic Synthesis and Materials Science*; VCH: Weinheim, Germany, 1995.
- (2) Long, N. J. *Angew. Chem., Int. Ed. Engl.* **1995**, *34*, 21.
- (3) Astruc, D. In *Electron Transfer and Radical Processes in Transition Metal Chemistry*; VCH: New York, 1995; Chapter 2.
- (4) Beer, P. D.; Smith, D. K. In *Progress in Inorganic Chemistry*; Karlin, K. D., Ed.; John Wiley: New York, 1997; Vol. 46, p 66.
- (5) Kingsborough, R. P.; Swager, T. M. In *Inorganic Chemistry*; Karlin, K. D., Ed.; John Wiley: New York, 1999; Vol. 48, p 123.
- (6) Kaifer, A. E. *Acc. Chem. Res.* **1999**, *32*, 62.
- (7) Omae, I. *Applications of Organometallic Compounds*; John Wiley: Chichester, U.K., 1998.
- (8) Briel, O.; Sünkel, K.; Krossing, I.; Nöth, H.; Schmälzlin, E.; Meerholz, K.; Bräuchle, C.; Beck, W. *Eur. J. Inorg. Chem.* **1999**, *3*, 483.
- (9) Boyd, P. D. W.; Burrall, A. K.; Campbell, W. D.; Cocks, P. A.; Gordon, K. C.; Jameson, G. B.; Officer, B. L.; Zhao, Z. *J. Chem. Soc., Chem. Commun.* **1999**, 637.
- (10) Christie, S. D.; Subramanian, S.; Thompson, L. K.; Zaworotko, M. J. *Chem. Soc., Chem. Commun.* **1994**, 2563.
- (11) Churchill, M. R.; Li, Y.-J.; Nalewajer, D.; Schaber, P. M.; Dorfman, P. M. *Inorg. Chem.* **1985**, *24*, 2684.
- (12) Abuhijleh, A. L.; Woods, C. J. *Chem. Soc., Dalton Trans.* **1992**, 1249.
- (13) Abuhijleh, A. L.; Pollitte, J.; Woods, C. *Inorg. Chim. Acta* **1994**, *215*, 131.
- (14) Costa, R.; López, C.; Molins, E.; Espinosa, E. *Inorg. Chem.* **1998**, *37*, 5686.

(15) Felthouse, T. R.; Laskowski, E. J.; Hendrickson, D. N. *Inorg. Chem.* **1977**, *16*, 1077.

(16) Costa, R.; García, A.; Ribas, J.; Mallah, T.; Journaux, Y.; Slatten, J.; Solans, X.; Rodriguez, V. *Inorg. Chem.* **1993**, *32*, 3733 and references therein.

(17) Julve, M.; Verdager, M.; Gleizes, A.; Philoche-Levissalles, M.; Kahn, O. *Inorg. Chem.* **1984**, *22*, 358.

(18) Journaux, Y.; Sletten, J.; Kahn, O. *Inorg. Chem.* **1985**, *24*, 4063.

environment around the metal atom and/or the mode of coordination of the ferrocenecarboxylate(−I) groups; these two factors are specially significant to determine the magnetic properties of Cu(II) compounds.^{19,20}

In this paper we report the syntheses and the study of the magnetic behavior of a novel Cu(II) polymetallic complex containing simultaneously the ferrocenecarboxylate(−I) ligand and the dipropylenetriamine (dpt) terminal group. It has been structurally characterized by X-ray analysis, showing a [Cu₂{(μ-O₂C)[(η⁵-C₅H₄)Fe(η⁵-C₅H₅)]₂}²⁺ tetrametallic core, and susceptibility measurements on it indicated ferromagnetic behavior. Ab initio DFT calculations on a simplified model have permitted us to obtain qualitative and fairly good quantitative approximations to their superexchange coupling constant.

Experimental Section

Materials. Ferrocenecarboxylic acid, the amine dpt, and Cu(ClO₄)₂·6H₂O were purchased from Aldrich and used as received. Sodium ferrocenecarboxylate was prepared as described previously.²¹ Methanol used as solvent was HPLC grade.

Safety Note: Caution! Perchlorate salts of metal complexes are potentially explosive. Only a small amount of material should be used, and this should be done with caution.

Synthesis of [Cu₂(dpt)₂{(μ-O₂C)[(η⁵-C₅H₄)Fe(η⁵-C₅H₅)]₂}(ClO₄)₂ (1). A solution containing 103 mg (1 mmol) of dipropylentriamine in methanol (5 cm³) was added slowly to a solution formed by 370 mg (1 mmol) of Cu(ClO₄)₂·6H₂O. Once the addition had finished, sodium ferrocenecarboxylate (252 mg, 1 mmol) dissolved in 10 cm³ of methanol was added. The reaction mixture was stirred at room temperature for 20 additional minutes. After this period the undissolved materials were removed by filtration and discarded. Evaporation of the filtrate produced green crystals of **1**. Yield: 450 mg, 43%. Anal. Calcd for C₃₄H₅₂N₆O₁₂-Cu₂Fe₂Cl₂ (found): C, 39.02 (38.7); H, 5.01 (4.9); N, 8.03 (8.0). $\bar{\nu}_{\max}/\text{cm}^{-1}$: (N-H) 3329–3232; (C-H) 2960–2860; (COO) 1548, 1464, 1382, and 1335; (ClO₄[−]) 1145, 1106, and 1087. When the synthesis of **1** is performed in the presence of humidity, water molecules are included in the solid, yielding a microcrystalline product whose chemical analysis agrees with the formulation [Cu(dpt)(H₂O){O₂C(η⁵-C₅H₄)Fe(η⁵-C₅H₅)](ClO₄). Anal. Calcd for C₁₇H₂₈N₃O₇CuFeCl (found): C, 37.72 (37.7); H, 5.21 (5.3); N, 7.76 (7.7). Their infrared spectrum is very similar to that of **1** except for a higher relative intensity of the 3330 cm^{−1} band. The microcrystalline samples show a temperature-independent paramagnetic behavior with a $\chi_m T$ value of 0.43 cm³ K mol^{−1} per Cu(II) ion, and no clue of any half-field signal is found in their EPR spectra.

X-ray Structure Determination. A green crystal of **1** (0.31 mm × 0.33 mm × 0.42 mm) was mounted on a Enraf-Nonius CAD4 four-circle diffractometer. Unit cell parameters were determined from automatic centering of 22 reflections (13° < θ < 18°). Compound **1** was found to crystallize in the monoclinic system. Intensities were collected with a graphite monochromated Mo Kα radiation of λ = 0.710 73 Å using ω-2θ scan technique with a θ range of 2.84–30.38°. Three reflections were measured every 2 h as orientation and intensity control, and no significant intensity decay was observed. Crystal data and experimental conditions are listed in Table 1.

A total of 6280 reflections were collected (6087 unique, $R_{\text{int}} = 0.0655$). The structure was solved by direct methods and refined using full matrix least-squares on F^2 . The function minimized was $\sum w(|F_o|^2 - |F_c|^2)^2$ where $w = [\sigma^2(|F_o|^2) + (0.0958P)^2]^{-1}$ and $P = [(|F_o|^2 + 2|F_c|^2)/3]$. f , f' , and f'' were obtained from the literature.²² Thermal motions of non-hydrogen atoms were refined anisotropically; H atoms were refined with a global isotropic thermal factor and positioned at

Table 1. Crystallographic Data for **1**

empirical formula	C ₃₄ H ₅₂ Cl ₂ Cu ₂ Fe ₂ N ₆ O ₁₂	$V, \text{Å}^3$	2018.6(6)
fw	1046.51	Z	2
space group	$P2_1/n$ (No. 14)	temp, K	293(2)
$a, \text{Å}$	9.920(2)	$\rho_{\text{calcd}}, \text{g cm}^{-3}$	1.722
$b, \text{Å}$	12.925(2)	μ (Mo Kα), mm ^{−1}	1.945
$c, \text{Å}$	15.768(3)	R1 [$I > 2\sigma(I)$] ^a	0.0575
β , deg	93.17(1)	wR2 [$I > 2\sigma(I)$] ^b	0.1377

$$^a R1 = \sum |F_o - F_c| / \sum |F_o|. \quad ^b wR2 = [\sum w(F_o^2 - F_c^2)^2 / \sum w(F_o^2)]^{1/2}.$$

calculated distances, with the exception of H(3), H(4), H(5), and H(6), whose coordinates were refined. The final R factors were $R1 = 0.0575$ and $wR2 = 0.1377$ for $I > 2\sigma(I)$, and the goodness-of-fit was 0.932 for all observed reflections. The number of refined parameters was 275. Maximum and minimum peaks in final difference synthesis were 1.146 and -1.008 e Å^{-3} . All calculations were performed using the SHELX-97 package.²³

Physical Measurements. Elemental analyses (C, H, and N) were carried out at the Institut de Química Bio-Orgànica, C.S.I.C. (Barcelona). Infrared spectra were recorded in the range 4000–400 cm^{−1} with a Nicolet Impact 400 using KBr pellets. Magnetic and EPR measurements were carried out in the Servei de Magnetoquímica, Universitat de Barcelona. Susceptibility measurements were carried out in the 300–8 K temperature range on powdered samples with a Manics-DSM8 pendulum type magnetometer equipped with a Drusch-EAF-16UE electromagnet working at 1.6 T and an Oxford helium continuous-flow cryostat. Crystals of complex **1** belonging to the sample used for X-ray structure determination were selected and crushed on an agate mortar. A total of 71.88 mg of the solid sample was placed using nonmetallic tools on the plastic container that had been calibrated at the same field and temperatures. Diamagnetic corrections were evaluated from Pascal's constants. The same sample was used to record the solid and solution EPR spectra, which were measured at X-band frequency (9.78 GHz) with a Bruker ES-200 spectrometer in the temperature range 300–4 K.

Computational Details. All calculations were carried out using the Gaussian 94 suite of programs²⁴ implemented on several workstations. The 6-3111+g basis were used for the metal centers and the 6-31g* basis sets for the remaining atoms. Single-point runs were carried out on a Power Indigo 2 machine. Geometry optimization required the use of a more powerful HP J282 computer.

Results and Discussion

Description of the Crystal Structure. The structure of complex **1** consists of discrete dinuclear [Cu₂(dpt)₂{(μ-O₂C)-[(η⁵-C₅H₄)Fe(η⁵-C₅H₅)]₂}²⁺ cations and perchlorate anions. The molecular structure of the dimeric ion is depicted in Figure 1 along with its labeling scheme. Main bond lengths and angles are given in Table 2.

The cation consists of two [Cu(dpt){O₂C(η⁵-C₅H₄)Fe(η⁵-C₅H₅)-O]⁺ fragments related by an inversion center where the ferrocenecarboxylate(−I) anions have become bridging ligands by forming a fifth coordination bond between the copper atom of one unit and the free carboxylate oxygen of their symmetric moiety. This results in a [Cu{(μ-O₂C)[(η⁵-C₅H₄)Fe(η⁵-C₅H₅)]-O''}]₂²⁺ core where the metals and the oxygen atoms form a puckered six-membered ring (Figure 2a) with a chair

(23) Sheldrick, G. M. *SHELXS97 and SHELXL97, Programs for the Solution and Refinement of Crystal Structures*; University of Göttingen: Göttingen, Germany, 1997.

(24) Frisch, M. J.; Trucks, G. W.; Schlegel, H. B.; Gill, P. M. W.; Johnson, B. G.; Robb, M. A.; Cheeseman, J. R.; Keith, T.; Petersson, G. A.; Montgomery, J. A.; Raghavachari, K.; Al-Laham, M. A.; Zakrzewski, V. G.; Ortiz, J. V.; Foresman, J. B.; Cioslowski, J.; Stefanov, B. B.; Nanayakkara, A.; Challacombe, M.; Peng, C. Y.; Ayala, P. Y.; Chen, W.; Wong, M. W.; Andres, J. L.; Replogle, E. S.; Gomperts, R.; Martin, R. L.; Fox, D. J.; Binkley, J. S.; Defrees, D. J.; Baker, J.; Stewart, J. P.; Head-Gordon, M.; Gonzalez, C.; Pople, J. A. *Gaussian 94*, revision E.1; Gaussian, Inc.: Pittsburgh, PA, 1995.

(19) Willet, R. D.; Gatteschi, D.; Kahn, O., Eds. *Magneto-Structural Correlations in Exchange Coupled Systems*; NATO ASI Series, Series C, 140; D. Reidel: Dordrecht, The Netherlands, 1985.

(20) Kahn, O. *Molecular Magnetism*; VCH Publishers: New York, 1993.

(21) *Gmelin Handbook of Inorganic Chemistry. Organoniron Compounds*; Springer-Verlag: Berlin, Germany, 1976; Vol. A3, p 58.

(22) *International Tables of X-ray Crystallography*; Kynoch Press: Birmingham, U.K., 1994; Vol. IV, pp 99–100, 149.

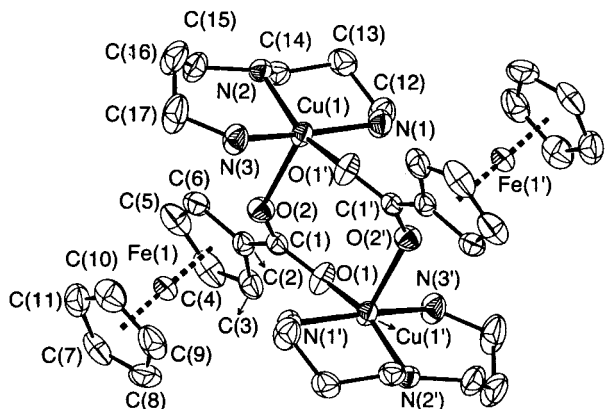


Figure 1. Molecular structure and atom labeling scheme of the dinuclear cation of $[\text{Cu}_2(\text{dpt})_2\{(\mu\text{-O}_2\text{C})[(\eta^5\text{-C}_5\text{H}_4)\text{Fe}(\eta^5\text{-C}_5\text{H}_5)]_2\}](\text{ClO}_4)_2$ (**1**).

Table 2. Selected Bond Distances (Å) and Angles (deg) for $[\text{Cu}_2(\text{dpt})_2\{(\mu\text{-O}_2\text{C})[(\eta^5\text{-C}_5\text{H}_4)\text{Fe}(\eta^5\text{-C}_5\text{H}_5)]_2\}](\text{ClO}_4)_2$ (**1**) with Their Estimated Standard Deviations in Parentheses

Cu(1)–O(1)	2.270(3)	Cu(1)–O(1') ^a	1.988(3)
Cu(1)–N(1)	2.008(4)	Cu(1)–N(2)	2.051(3)
Cu(1)–N(3)	2.025(3)	O(1)–C(1)	1.272(5)
O(2)–C(1)	1.253(5)	C(1)–C(2)	1.484(5)
Fe(1)–C _{ring} ^b	2.042(11)	C _{ring} –C _{ring} ^b	1.421(25)
N(1)–Cu(1)–N(2)	92.04(14)	N(1)–Cu(1)–N(3)	166.51(16)
N(2)–Cu(1)–N(3)	94.80(14)	N(1)–Cu(1)–O(1') ^a	89.11(13)
N(1)–Cu(1)–O(2)	100.78(14)	N(2)–Cu(1)–O(1') ^a	159.02(14)
N(2)–Cu(1)–O(2)	91.84(12)	N(3)–Cu(1)–O(1') ^a	80.37(14)
N(3)–Cu(1)–O(2)	90.62(14)	O(1') ^a –Cu(1)–O(2)	108.52(12)
Cu(1)–O(1') ^a –C(1') ^a	131.6(3)	Cu(1)–O(2)–C(1)	136.5(3)
O(1)–C(1)–O(2)	125.1(4)	O(1)–C(1)–C(2)	115.6(4)
O(2)–C(1)–C(2)	119.3(4)		

^a Under symmetry operations $-x, -y, -z$. ^b Average value for the ferrocenyl moieties.

conformation due to the syn, anti binding of the carboxylato groups (see Figure 2b). The Cu \cdots Cu intradimer distance is 4.301(1) Å, clearly larger than those reported in the two dinuclear cations of complex $[\text{Cu}_2(\text{bpy})_2\{(\mu\text{-O}_2\text{C})[(\eta^5\text{-C}_5\text{H}_4)\text{Fe}(\eta^5\text{-C}_5\text{H}_5)]_2\}](\text{ClO}_4)(\text{CH}_3\text{OH})][\text{Cu}_2(\text{bpy})_2\{(\mu\text{-O}_2\text{C})[(\eta^5\text{-C}_5\text{H}_4)\text{Fe}(\eta^5\text{-C}_5\text{H}_5)]_2\}(\text{CH}_3\text{OH})_2](\text{ClO}_4)_3$,¹⁴ in which the ferrocenecarboxylato bridges and the Cu(II) ions form six-membered rings, which adopt the boat conformation.

The copper atoms have a 4 + 1 square-pyramidal coordination, their basal planes being formed by the three nitrogens {N(1), N(2), and N(3)} of the tridentate amine and the oxygen O(1') belonging to one ferrocenecarboxylato (–I) ligand. All the donor atoms are less than 0.11 Å away from their least-squares plane, and the Cu(1) deviates from this plane by 0.27 Å toward the apical position, which is occupied by the O(2) atom from the other carboxylate at 2.270(3) Å of the metal. The coordination geometry is confirmed by the evaluation of both Addison's parameter²⁵ ($\tau = 0.12$) and a Holmes' pseudorotation percentage²⁶ of 18% (from sp to tbp).

The central fragment [O(1), O(2), O(1'), O(2')] of the cation is nearly planar, and the O(2), Cu(1), and O(1') atoms form a dihedral angle of 50.4° with it. The carboxylate groups, with a bite angle of 125.1(4)°, are not strictly coplanar with the former plane, leading to a dihedral angle of 13.1°. The torsion angle Cu(1)–O(2)–O(1)–Cu(1') is 58.2°.

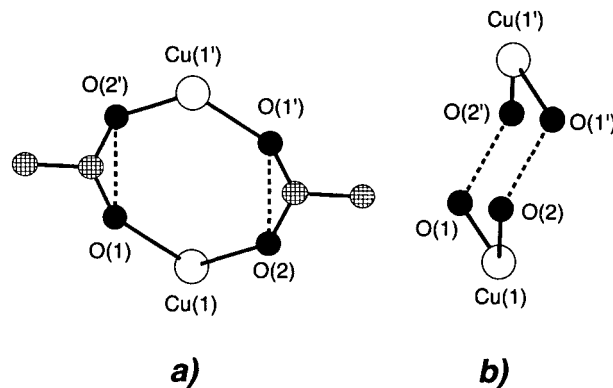


Figure 2. Alternative representations of the central core of $[\text{Cu}_2(\text{dpt})_2\{(\mu\text{-O}_2\text{C})[(\eta^5\text{-C}_5\text{H}_4)\text{Fe}(\eta^5\text{-C}_5\text{H}_5)]_2\}](\text{ClO}_4)_2$ (**1**): (a) view along the S_2 axis, showing the six-membered ring formed by the copper ions and the oxygen atoms; (b) lateral view displaying the ring's chair conformation. Ferrocenyl moieties have been omitted for clarity.

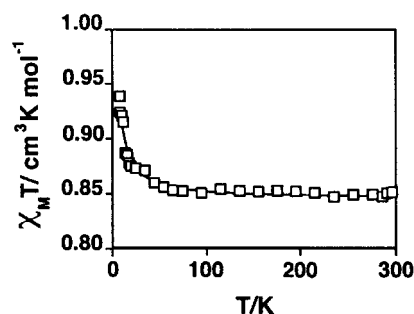


Figure 3. Temperature dependence of the $\chi_m T$ product for a polycrystalline sample of $[\text{Cu}_2(\text{dpt})_2\{(\mu\text{-O}_2\text{C})[(\eta^5\text{-C}_5\text{H}_4)\text{Fe}(\eta^5\text{-C}_5\text{H}_5)]_2\}](\text{ClO}_4)_2$ (**1**). The solid line represents the fit of the data.

Bond lengths and angles involving the $(\eta^5\text{-C}_5\text{H}_5)\text{Fe}(\eta^5\text{-C}_5\text{H}_4)$ unit are consistent with those reported in the literature.²⁷ The pentagonal rings of the ferrocenyl fragments are planar and nearly parallel (tilt angle: 3.4°), deviating from the eclipsed conformation by 16.0°. The dihedral angle between the carboxylate group and its C_5H_4 bonded ring is 8.8°. The minimum distance between Cu and Fe atoms is 5.5335(13) Å for Cu(1) and Fe(1').

Magnetic Studies. The magnetic behavior of compound **1** is shown in Figure 3 as a plot of $\chi_m T$ vs T . At room temperature, the $\chi_m T$ product is equal to 0.85 $\text{cm}^3 \text{K mol}^{-1}$, which is the expected value for two uncoupled copper(II) ions. This value remains stable up to 70 K and then progressively increases upon cooling, reaching a value of 0.93 $\text{cm}^3 \text{K mol}^{-1}$ at 8.0 K. This behavior is characteristic of a weak ferromagnetic coupling between the two copper(II) ions; the ground triplet state is the only significantly populated at very low temperatures, leading to an increase in the $\chi_m T$ product. The results are well interpreted using the Bleaney–Bowers equation.²⁸ A least-squares fitting procedure leads to a triplet–singlet gap of +2.5(3) cm^{-1} and a g value of 2.12(1), with an agreement factor defined as $\sum[(\chi_m T)_{\text{calcd}} - (\chi_m T)_{\text{obsd}}]^2 / \sum[(\chi_m T)_{\text{obsd}}]^2$ of 5.2×10^{-5} . The powder EPR spectra of **1** recorded under routine conditions in the 4–293 K range show a unique, broad, and unresolved signal centered at 3225 G, which corresponds to a g value of 2.16, fairly close to that obtained from the magnetic data. When the microwave power and receiver gain were raised, a very weak half-field resonance was observed at 1595 G near the low-field

(25) Addison, A. W.; Rao, T. N.; Reedijk, J.; van Rijn, J.; Verschoor, G. C. *J. Chem. Soc., Dalton Trans.* **1984**, 2349.

(26) Holmes, R. R. *Prog. Inorg. Chem.* **1984**, 32, 119.

(27) Allen, T. H.; Kennard, O. *Chem. Design. Automat. News* **1993**, 8, 146.

(28) Bleaney, B.; Bowers, K. D. *Proc. R. Soc. London, Ser. A* **1952**, 214.

side of the bump. As the relative intensity increases when temperature is lowered, it can be assigned to a $\Delta M_s = 2$ transition inside the ground triplet state, whose electronic population increases at low temperatures. The difficulty in detecting this feature is attributed to a very low value of the zero-field splitting parameter,^{29–31} which agrees with the nearly isotropic shape of the main signal.

When the solid sample is dissolved into acetonitrile, the half-field EPR signal is lost, suggesting a fragmentation of the dinuclear cation. Consequently, no other instrumental techniques in solution were considered.

Electronic Structure Calculations. The simplest theoretical approach to the magnetic behavior observed for the dinuclear compound **1** is the one based on the idea of Kahn's magnetic orbitals,²⁰ which are essentially a localized representation of the single occupied molecular orbital, SOMO. In this approach, the dinuclear cation is modeled by the superposition of two inversion-center-related $[\text{Cu}(\text{NH}_3)_3(\text{O}_2\text{CH})_2]$ fragments. The two $[\text{Cu}(\text{NH}_3)_3(\text{O}_2\text{CH})_2]$ moieties are superimposed in such a way that the carboxylato bridges in each fragment overlap so that only two of these ligands appear in the cationic $[\text{Cu}_2(\text{NH}_3)_6(\mu\text{-O}_2\text{CH})_2]^{2+}$ model (Figure 4). The magnetic orbital of this fragment is then obtained in a direct way by a suitable transformation of the delocalized canonical molecular orbitals of one of these moieties. In practice, *ab initio* unrestricted open-shell calculations, either unrestricted Hartree–Fock or unrestricted Kohn–Sham, are carried out for the lowest doublet state of the chosen fragment. The canonical molecular orbitals are then transformed to natural molecular orbitals, NMO, by explicit diagonalization of the first-order density matrix. In the natural orbital basis the unpaired spin density belongs entirely to the SOMO, which indeed appears to be localized mainly around the metal center.

A first qualitative idea about the magnitude of the magnetic coupling may be obtained from the analysis of the spin density in the metal center and bridging ligands. In the Cu atoms the spin density lies almost entirely in the d_{xy} atomic orbital. The main carboxylato contribution arises from the basal-bonded oxygen atom, and no significant spin density in the rest of the ligand is found (see Figure 5). When the two fragments are superimposed to form the dinuclear cation $[\text{Cu}_2(\text{NH}_3)_6(\mu\text{-O}_2\text{CH})_2]^{2+}$, both NMO have the spin density located in two parallel planes that do not contain the bridging ligands (Figure 6). From a qualitative point of view one expects that this orientation minimizes their interaction, thus resulting in a small singlet–triplet gap. The interaction topology is similar to that reported by Kahn³² for the cations $[\text{Cu}_2(\text{tmen})_2(\text{L})_2(\mu\text{-C}_2\text{O}_4)]^{2+}$. When $\text{L} = \text{H}_2\text{O}$, the basal planes of the copper coordination pyramid and the bridging oxalato are coplanar and the coupling is strongly antiferromagnetic; when $\text{L} = 2\text{-methylimidazole}$, the basal planes are parallel and the oxalato bridge lies perpendicular to them. In this case the interaction is only weakly antiferromagnetic, as one would expect from the reduced overlap between the magnetic and ligand orbitals. In the limit of very small overlap the direct exchange may dominate and the latter situation can lead to a weak ferromagnetic interaction. Conse-

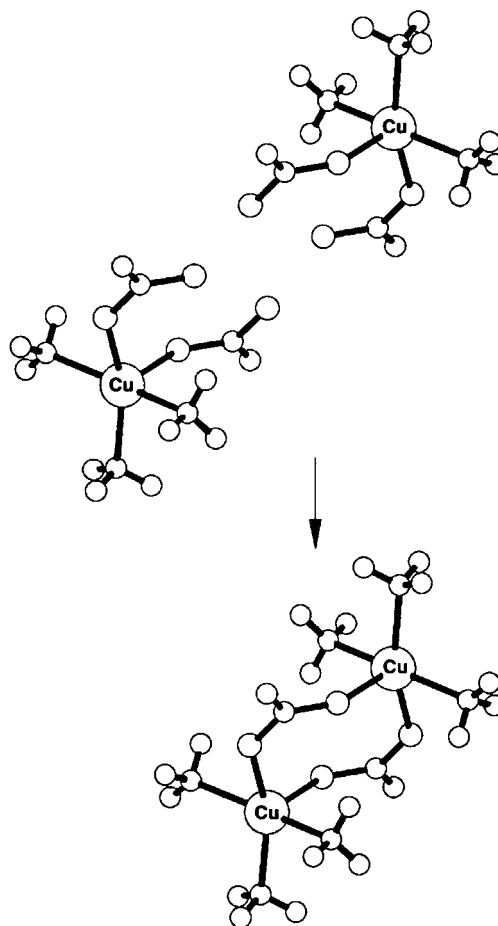


Figure 4. Schematic representation of the assembly of two mononuclear $[\text{Cu}(\text{NH}_3)_3(\text{O}_2\text{CH})_2]$ fragments, containing copper(II) ions in a square-pyramidal coordination, to give the dinuclear $[\text{Cu}_2(\text{NH}_3)_6(\mu\text{-O}_2\text{CH})_2]^{2+}$ model of the cation of compound **1**.

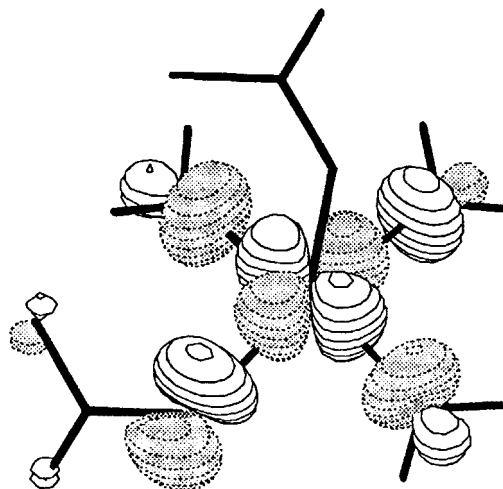


Figure 5. Magnetic orbital of the mononuclear $[\text{Cu}(\text{NH}_3)_3(\text{O}_2\text{CH})_2]$ fragment obtained from DFT calculations.

quently, the procedure described above permits the identification of the magnetic orbitals, which are mainly responsible for magnetic coupling but does not bring any information about its magnitude. Therefore, from the analysis of the experimental geometric structure of **1** and of their molecular orbitals, it is very difficult to interpret the experimental magnetic measurements. Hence, a proper explanation of magnetic coupling of **1** has to be based on accurate *ab initio* calculations of the singlet–

(29) Abragam, A.; Bleaney, B. *EPR of Transition Ions*; Oxford University Press: London, 1970.

(30) Comarmond, J.; Plumere, P.; Lehn, J. M.; Agnus, Y.; Louis, R.; Weiss, R.; Kahn, O.; Morgenstern-Badarau, I. *J. Am. Chem. Soc.* **1982**, *104*, 6330.

(31) Tirado-Guerra, S.; Cuevas-Garibay, N. A.; Sosa-Torres, M. E.; Zamorano-Ulloa, R. *J. Chem. Soc., Dalton Trans.* **1998**, 2431.

(32) Julve, M.; Verdaguier, M.; Gleizes, A.; Philoche-Levisalles, M.; Kahn, O. *Inorg. Chem.* **1984**, *23*, 3808.

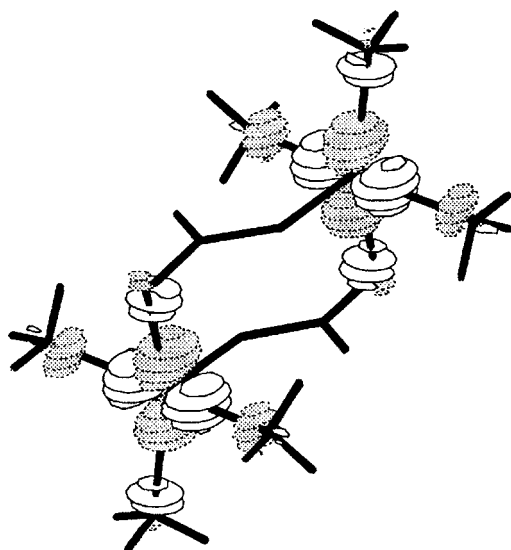


Figure 6. Symmetric magnetic orbital for the triplet state of the dinuclear $[\text{Cu}_2(\text{NH}_3)_6(\mu\text{-O}_2\text{CH})_2]^{2+}$ model of the cation of compound **1**, displaying the orthogonality of the magnetic orbitals of the mononuclear fragments.

triplet gap. In principle, the singlet–triplet gap should be computed from a proper configuration interaction approach.³³ However, the large size of the system, even using a simplified representation of the ligands, prevents the use of this methodology. An alternative, yet efficient, method consists of using the broken-symmetry (BS) approach at either the UHF or DFT levels of theory.^{34,35} In this methodology, the triplet, $|T\rangle$, and singlet, $|S\rangle$, states are approximately represented by a single spin-unrestricted determinant. For the triplet state it is always possible to use a single determinant wave function, which is indeed a proper pure spin eigenfunction (except for the small spin contamination arising from the use of an unrestricted formalism). However, in the case of a singlet state arising from two electrons in two open-shell, magnetic orbitals, it is necessary to use a linear combination of the two possible determinants, $|\alpha\beta\rangle$ and $|\beta\alpha\rangle$, to obtain a pure spin state. In the broken-symmetry approach one chooses to minimize the energy of one of these two determinants, and consequently, the final state does not represent any pure spin state. However, it is possible to relate the energy of this BS solution with that of the pure singlet.³⁵ The BS state can be viewed as the weighted average of the $|T\rangle$ and $|S\rangle$ states, and the singlet–triplet gap can be then calculated as

$$E(|T\rangle) - E(|S\rangle) = 2\{E(|T\rangle) - E(|BS\rangle)\}$$

The very large size of **1** makes it very difficult to carry ab initio calculations even in the computationally simplified broken-symmetry approach. In this case, the use of a model system is unavoidable. The first preliminary model was chosen to be the $[\text{Cu}_2(\text{NH}_3)_6(\mu\text{-O}_2\text{CH})_2]^{2+}$ cation. However, geometry optimizations on the triplet state using the hybrid B3LYP exchange–correlation functional of DFT^{36,37} resulted in a distortion of the core of the molecule to allow the formation of two intramo-

lecular $\text{O}\cdots\text{H}-\text{N}$ hydrogen bonds. This unexpected effect could only arise from the excessive simplification of the model. Therefore, the process was repeated on the $[\text{Cu}_2(\text{dpt})_2(\mu\text{-O}_2\text{CH})_2]^{2+}$ cation. The calculation, which involved 62 atoms, 500 basis functions, and 938 primitive Gaussian functions, also gave a similar disappointing result. A revision of the molecular movements favored in the geometry optimization processes showed that they would correspond to a wide rotation of the ferrocenyl moieties around the Cu–Cu axis. Here, one must realize that although the deformation of the molecule in the gas-phase calculations is favorable, there is no space available to allow these displacements in the crystal network. To reproduce as accurately as possible the solid-state magnetic behavior, subsequent calculations were carried out at crystallographic geometry on the simplified $[\text{Cu}_2(\text{NH}_3)_6(\mu\text{-O}_2\text{CH})_2]^{2+}$ model. Recent work on wide-gap insulators has shown that this is indeed a very good approach.^{38–41}

Self-consistent field (SCF) calculations were then performed on the dinuclear model with an energy convergence threshold up to 10^{-9} hartree, using both UHF and B3LYP wave functions. The resulting coupling constants were $+0.12$ and $+3.89$ cm^{-1} , respectively. Both methods account for the experimentally observed ferromagnetic coupling, although the calculated value is underestimated in the former and overestimated in the latter. This is in agreement with the treatment of the electronic correlation of both model chemistries; Hartree–Fock neglects these effects, whereas the density functional enhances them.^{42,43} The use of an equivalent mixing of Hartree–Fock and Becke gradient-corrected exchange functional⁴⁴ together with the LYP³⁷ correlation functionals affords a singlet–triplet gap of $+0.62$ cm^{-1} , closer to the experimental value. Although the choice of a given exchange–correlation functional affects the calculated coupling constant,^{38–43} the results obtained agree in predicting a weakly ferromagnetic behavior and provide higher and lower bounds to the calculated value.

Conclusions

As expected, the complexation with dipropylenetriamine induces square-pyramidal pentacoordination around the copper(II) ion in compound **1**. Three basal sites are occupied by the nitrogen atoms of each amine. Besides that, the metal bonds tightly to one of the oxygen atoms of the ferrocenecarboxylato ligand, O(1), which lies on the vacant basal position. The occupancy of the apical site, which will determine the mode of coordination of the carboxylato ligand, is governed by the basicity of the available O donors and the steric effects induced by both the substituents on the N-donor atoms of the triamine and the ferrocenyl moieties of the carboxylato ligands. The terminal $-\text{NR}_2$ groups of dpt are the smallest possible ($\text{ES}-\text{CH}$ of 1.00 for $-\text{NH}_2$).⁴⁵ Thus, the large free space around the Cu(II) allows the approach of another ferrocenecarboxylato ligand from a second $[\text{Cu}(\text{dpt})\{\text{O}_2\text{C}(\eta^5\text{-C}_5\text{H}_4)\text{Fe}(\eta^5\text{-C}_5\text{H}_5)\}]^+$ unit that forms a weak $\text{O}(2')-\text{Cu}(1)$ bond in the apical position,

(33) Illas, F.; Moreira, I. d. P. R.; de Graaf, C.; Barone, V. *Theor. Chem. Acc.* **2000**, *104*, 265.

(34) Noodleman, L.; Peng, C. Y.; Case, D. A.; Mousesda, J. M. *Coord. Chem. Rev.* **1995**, *144*, 199.

(35) Caballol, R.; Castell, O.; Illas, F.; Malrieu, J. P.; Moreira, I. d. P. R. *J. Phys. Chem.* **1997**, *42*, 77860.

(36) Becke, A. D. *J. Chem. Phys.* **1993**, *98*, 5648.

(37) Lee, C.; Yang, W.; Parr, R. G. *Phys. Rev. B* **1982**, *37*, 785.

(38) Moreira, I. d. P. R.; Illas, F. *Phys. Rev. B* **1999**, *60*, 5179.

(39) Reinhardt, P.; Habas, M. P.; Dovesi, R.; Moreira, I. d. P. R.; Illas, F. *Phys. Rev. B* **1999**, *59*, 1016.

(40) Calzado, C. J.; Sanz, J. F.; Malrieu, J. P.; Illas, F. *Chem. Phys. Lett.* **1999**, *307*, 102.

(41) De Graaf, C.; Moreira, I. d. P. R.; Illas, F.; Martin, R. L. *Phys. Rev. B* **1999**, *60*, 3457.

(42) Martin, R. L.; Illas, F. *Phys. Rev. Lett.* **1997**, *79*, 1539.

(43) Illas, F.; Martin, R. L. *J. Chem. Phys.* **1998**, *108*, 2519.

(44) Becke, A. D. *Phys. Rev. A* **1998**, *38*, 3098.

(45) Hansch, C.; Leo, A.; Hoekman, D. *Exploring QSAR. Hydrophobic, Electronic and Steric Constants*; ACS Professional Reference Books: Washington, DC, 1995.

resulting in the orthogonality of the magnetic orbitals of both the d^9 ions that leads to a ferromagnetic interaction. This is expected to be very weak because the basal faces of the copper coordination polyhedra, which contain the chief spin density, lie in parallel but separated planes.

Ab initio calculations predicted ferromagnetic coupling in **1**, although the exact experimental value has not been properly reproduced by any of the methods used. The DFT results can be considered the upper and the lower limits of a 3.3 cm^{-1} wide theoretical interval, with the experimental gap value placed at its center.

To sum up, the results reported in this work show not only the high versatility of ferrocenecarboxylato ligand but also the importance of the nature of the N-donor ligand in determining both the formation of dimeric systems and their magnetic properties. Keeping in mind the uncertainty inherent in the

experimental determination of weak ferromagnetic coupling constants, the complementary use of theoretical ab initio calculations helps to unequivocally characterize the first ferromagnetic Cu(II) complex containing two ferrocenecarboxylate anions as bridging ligands.

Acknowledgment. R.C., C.L., and F.I. thank the Ministerio de Educación y Cultura for financial support (Grants PB096-0163, PB096-0164, and PB98-1216-CO2-01, respectively).

Supporting Information Available: One X-ray crystallographic file, in CIF format, for complex **1**; Figure S1 showing the variable temperature EPR powder spectra of **1** in the half-field resonance region. This material is available free of charge via the Internet at <http://pubs.acs.org>.

IC000521N